ARTICLE

Check for updates

Revised Storegga Slide reconstruction reveals two major submarine landslides 12,000 years apart

Jens Karstens [1]✉, Haflidi Haflidason [2], Christian Berndt [1] & Gareth J. Crutchley[1]

The Storegga Slide is the largest known exposed submarine landslide in the world, which triggered a tsunami that inundated the coasts of northern Europe ~8,150 years ago. Previous studies suggested the removal of 50–70 m of sediment from the northern slide scar segment, contributing half of the total slide volume of up to 3200 km³. However, new sediment echosounder profiles and sedimentological constraints show that most material within the northern Storegga slide scar had already failed ~20,000 years ago, at the end of the Last Glacial Maximum. We refer to this previously undetected slope failure as the Nyegga Slide. In our revised slope failure reconstruction, the Nyegga Slide removed more than 35 m of sediments that were previously attributed to the tsunamigenic Storegga Slide. This implies that large slope failures at the mid-Norwegian margin occur more frequently than previously thought, indicating a higher tsunami hazard for the North Atlantic.

[1] GEOMAR Helmholtz Centre for Ocean Research Kiel, Kiel, Germany. [2] Department of Earth Science, University of Bergen, Bergen, Norway.
✉email: jkarstens@geomar.de

The 1929 Grand Banks earthquake triggered the most recent large-scale landslide on open continental slopes, incorporating 200 km³ of seafloor sediments, which caused a tsunami with run-up heights of up to 13 m on the Newfoundland coast[1]. Morphological analyses of the continental margins of the North Atlantic have revealed dozens of late-Quaternary slide scars associated with slope failures of even greater dimensions[2,3]. With an estimated volume of 2400 to 3200 km³, the Storegga Slide is the largest known continental margin slope failure, stretching approximately 300 km along the mid-Norwegian continental shelf-break and extending over 800 km into the Norway Basin[4]

(Fig. 1a). Previous analyses concluded that the Storegga Slide developed in multiple phases. The first phase initiated more than 100 km downslope from the headwall and developed retrogressively upslope, removing up to 50 m of poorly consolidated, glacial sediments from the northern half of the slide scar, which transformed into debris flows and turbidity currents and were deposited hundreds of kilometers away in the Norway Basin[4–6]. During the second phase, remaining sediments were affected by lateral spreading along a well-defined glide plane as well as some minor, local slope failures[6]. Finally, the central slide segment failed and incised several hundred meters deep into the
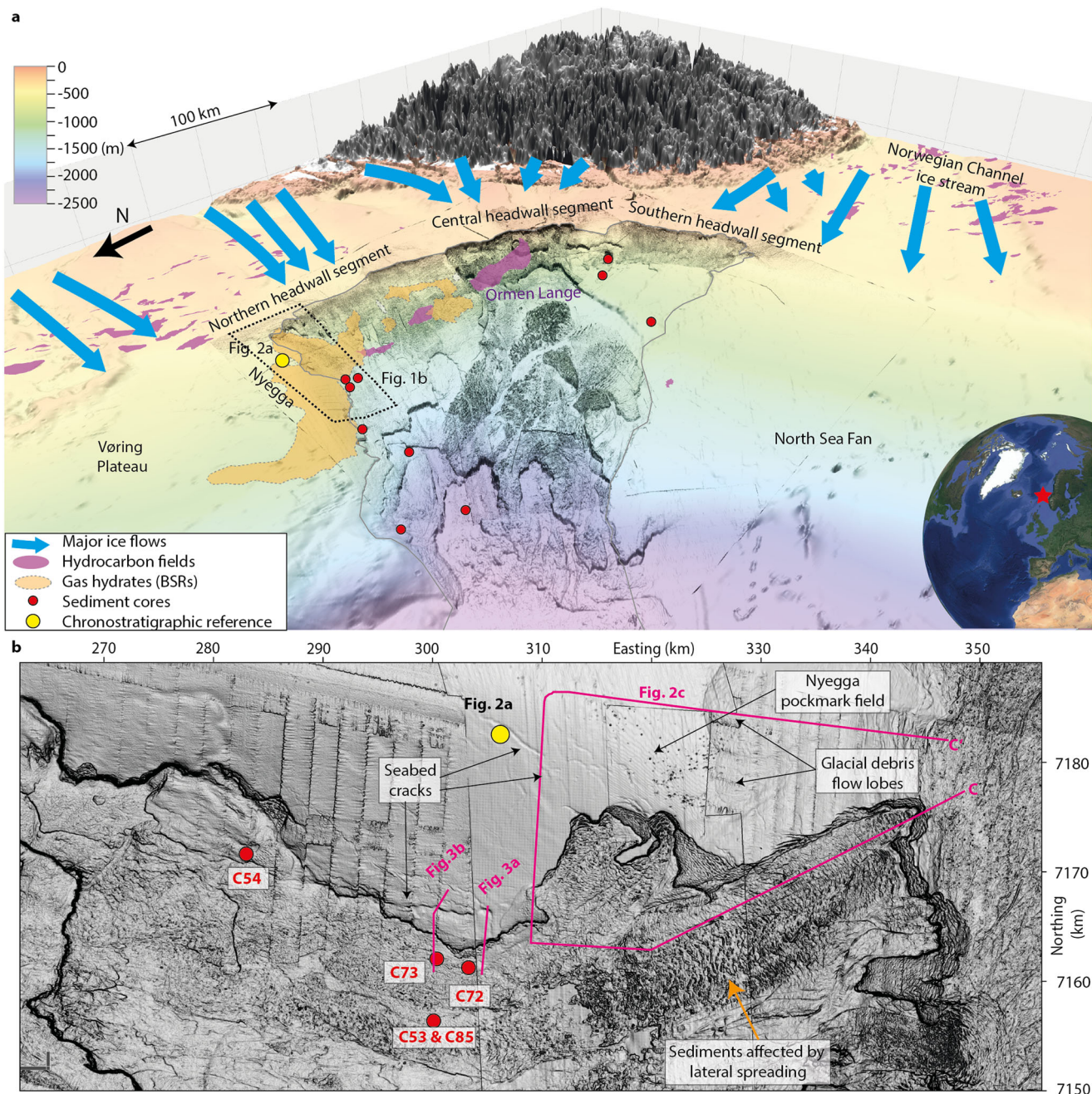

Fig. 1 The Storegga Slide Complex. a Perspective view onto the mid-Norwegian Margin with the Storegga Slide Complex and the neighbouring Vøring Plateau and Norwegian Channel. Red dots show the locations of cores that are inconsistent with the previously established reconstruction model of the Storegga Slide, and dashed black box indicates the area covered by sediment echosounder profiles. Globe illustration from Google Earth; Map data: SIO, NOAA, U.S. Navy, NGA, GEBCO, Landsat/Copernicus, IBCAO, U.S. Geological Survey. **b** Seafloor gradient map showing the north-eastern corner of the Storegga Slide Complex with echosounder profiles (magenta lines), sediment core locations (red dots) and the location of the reference age-depth model (yellow dot) in Fig. 2a; ref. [14].

substrate[4,6]. Based on seismically constrained pre-slide seafloor reconstructions, the first phase of the Storegga Slide mobilized ~1300 to 1600 km³, contributing 50% of the total slide volume, while lateral spreading and minor secondary slope failures added up to ~600 to 900 km³. The failure of the central slide segment involved ~500 to 800 km³ and is considered the main contributor to tsunami generation[7]. Radiocarbon dating of sediment cores from throughout the slide scar indicates that the Storegga Slide occurred around 8150 years before present (BP)[8]. This coincides with the age of tsunami deposits related to a tsunami with run-up heights of more than 20 m on the Shetland Islands and which affected coasts as distant as Denmark, Greenland and the Barents Sea coast[9–12].

Storegga is considered the best-studied mega slide complex worldwide and much of our understanding of large-scale slope failures derives from it. Additionally, the well-constrained tsunami is a benchmark for tsunami hazard assessments from submarine landslides. Here, we present new geophysical and sedimentological data of the north-eastern region of the Storegga Slide that prove that this part of the slide scar was affected by a previously unknown large-scale slope failure at the end of the Last Glacial Maximum (LGM), ~ 20,000 years BP. This discovery has major implications for the understanding of the Storegga Slide itself and, more broadly, for geohazard assessment related to continental margin slope failures.

Results

Seismostratigraphic evidence for the Nyegga Slide in echosounder profiles. Repeated ice-lobe advances during the LGM, and the decay of the Fennoscandian Ice Sheet, deposited more than 50 m of sediments during a relatively short period in the study area[13,14]. These deposits are preserved in the northern sidewall of the Storegga Slide (Fig. 2b, c). Several sediment cores from the southern Vøring Plateau define their chronostratigraphy at high spatial and temporal resolution (Fig. 2a) and constrain the age of the key horizons R1 to R7 in echosounder profiles[14]. However, due to a lack of datable sediment samples beneath R7, the age of the Storegga Slide glide plane (R8) is not well constrained, but it likely corresponds to the last interglacial (MIS 5e) ~120,000 years BP[13]. The combined echosounder and sediment core data show that glacial debris lobes were emplaced between 21,800 and 19,800 years BP (R3 to R5) and that more than 30 m of melt-water plume deposits have been deposited between 21,800 and 16,400 years BP (R1 to R5) (Fig. 2). The slide scar infill is acoustically transparent in echosounder data, with horizon R8 marking the slide plane of material affected by lateral spreading[6] (Fig. 2d). These deformed sediments are covered locally by a thin, acoustically transparent sediment veneer. In the intact sidewall segment, sediments above R8 in Fig. 2b have a thickness of ~120 ms TWT (90 m assuming a seismic velocity of 1,500 m/s). This constrains the pre-failure topography on the neighboring slope (dashed line in Fig. 2d) and enables a comparison of intact and failed slope segments. The comparison suggests that 50–70 m of sediment have been removed from the slide scar in the study area, as indicated by the black dashed line in Fig. 2d. The remaining sediments have been affected by lateral spreading during the Storegga Slide[4,6].

Echosounder profiles crossing the northern sidewall of the Storegga Slide show an acoustically transparent slide scar infill and an additional transparent unit representing a previously unknown mass-transport deposit (MTD) interbedded between well-stratified sediments (Fig. 3; labelled Nyegga Slide MTD). The MTD has a thickness of up to ~15 m and extends from the sidewall to a fault that correlates with a seafloor crack. Horizon R6 defines the base and R3 the top of the MTD, indicating that it

contains material deposited after 27,600 BP, which failed at about 20,000 years BP during the Nyegga Slide. Comparison with the unaffected sidewall stratigraphy indicates that this slide affected at least 20 m of the sediment column between horizons R3 to R6 (Fig. 3). However, at the time of the Nyegga Slide, stratigraphic units between horizons R3 to R8 extended into the area of the present-day slide scar (illustrated by the strata beneath R8 in Fig. 3). The observed deformation of the MTD indicates lateral movement that requires (at least partial) evacuation of the slide scar during or prior to the deposition of the MTD. Therefore, the ~20 m of sediments affected within the sidewall stratigraphy represent the minimum thickness of sediments that were removed during this event. The 30 m-thick undisturbed sediment cover rules out the possibility that the MTD represents material that could have been disturbed during the Storegga Slide. The NE Storegga Slide scar infill contains an internal boundary dividing the acoustically transparent sediments into two subunits, plus a thin transparent veneer of sediments at the top (Fig. 3). The internal boundary within the slide scar infill correlates with the topmost reflection of a block with intact internal stratification (Fig. 3a; see enlargements).

Chronostratigraphic evidence for the Nyegga Slide in sediment cores. As part of the 'Seabed' and 'Ormen Lange' projects[15], 89 sediment cores from throughout the Storegga Slide scar were collected and radiocarbon dated[4,8]. Most of the cores (especially from the central slide segment) terminated in a several meters thick MTD associated with the Storegga Slide. Dating of the sediments covering the Storegga Slide deposits puts the Storegga Slide at ~8150 BP[4,8]. While dating the sediments above the Storegga Slide deposit or discontinuity allows the failure age to be constrained, it does not provide insight into the magnitude of the slope failure (Fig. 4). In the absence of evidence to the contrary, the entire present-day slide-scar has previously been associated solely with the ~8150 BP event. However, there are sediment cores from the northern (and southern) slide segments that penetrate the Storegga Slide deposits or the associated Storegga discontinuity (SD in Fig. 4), thereby allowing the sediments beneath to be analysed. In combination with sediment echosounder observations of the Nyegga Slide, these cores enable a reassessment of the slide scar evacuation in relation to the ~20,000 BP and ~8150 BP events.

Previous reconstructions assumed that the initial phase of the Storegga Slide removed more than 50 m from the slide scar[6,8], which would have included all sediments younger than ~30,000 years, forming a failure plane expected between horizons R6 and R7 (Fig. 5). However, sediment core C72 contains sediments with an age of ~10,000 BP beneath the Storegga discontinuity and core C73 contains sediments with an age of ~18,000 BP (Fig. 5c, d). This cannot be reconciled with a scenario in which the 8150 BP Storegga Slide was the only slope failure event that contributed to the slide scar formation (Fig. 6a).

By accounting for the ~20,000 BP event, we can explain the presence of post-LGM sediments beneath the Storegga discontinuity. Moreover, a comparison between sidewall and slide scar stratigraphy allows the thickness of failed sediments to be constrained, using R8 as a reference surface. R8 is present beneath both the intact side wall and the slide scar. Deposition of sediments above R8 is considered to be uniform (crossing the present-day sidewall), and only mass movements during the ~20,000 BP and ~8,150 BP events are expected to have contributed to stratigraphic differences between the sidewall and the slide scar (Fig. 5a, b). Sediments with an age of ~18,600 BP (horizon R2) are located 55 to 57 m above R8 in the intact sidewall stratigraphy (Fig. 5a, b). Sediments of the same age are
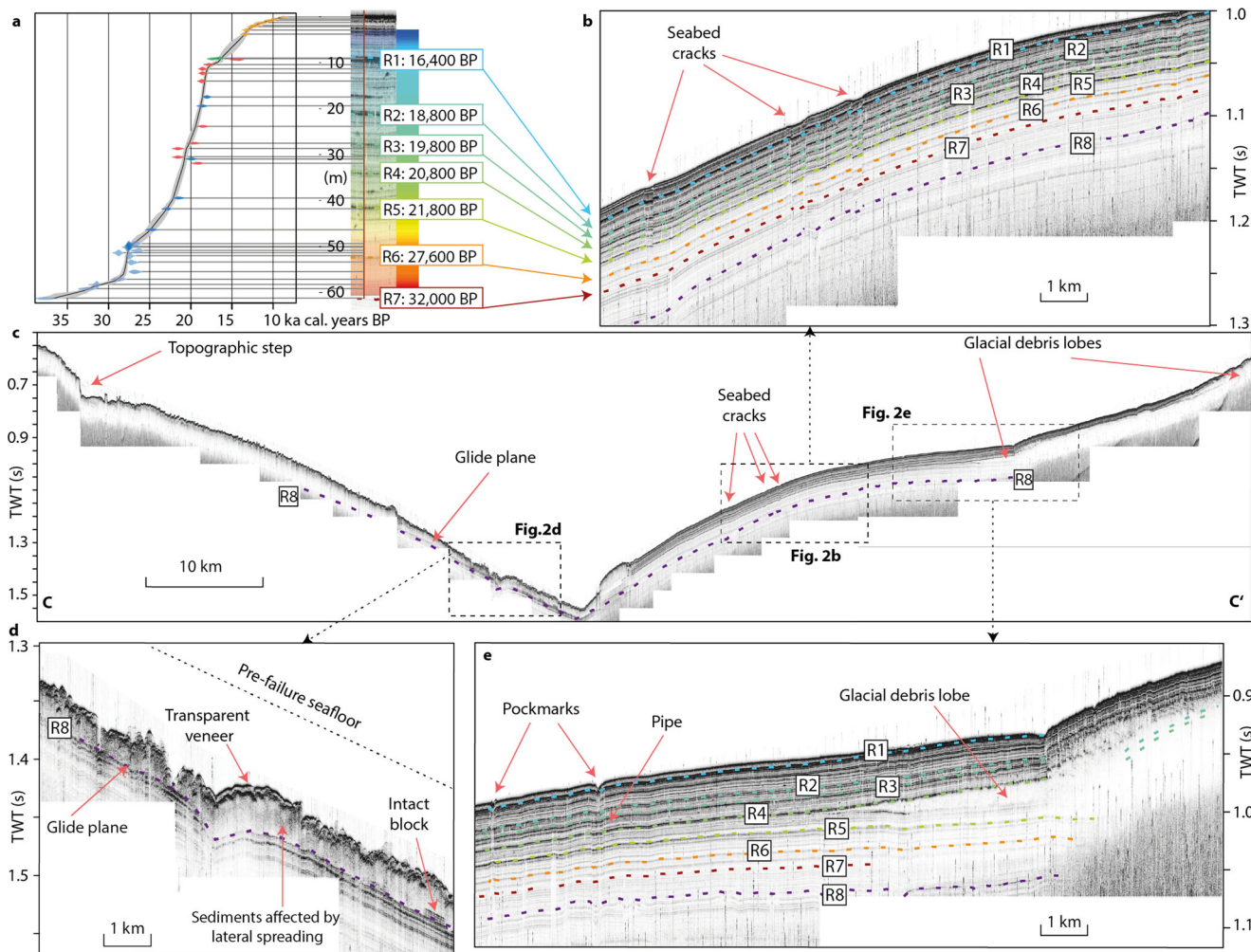
Fig. 2 Reference core chronostratigraphy and sediment echosounder profiles from the northern sidewall of the Storegga Slide. a Age-depth model for key horizons R1 to R7 for the northern sidewall of the Storegga Slide Complex from ref. [14]. **b** Echosounder profile showing the intact sidewall stratigraphy with key horizons R1 to R8 and seafloor cracks annotated. **c** Echosounder profile crossing the Storegga Slide and the intact side wall showing horizon R8, and the location of enlargements b, d and e. **d** Echosounder profile showing the chaotic, transparent sediments covering R8 with small intact block and a thin transparent veneer, the Storegga Slide glide plane, and the extrapolated pre-Storegga seafloor depth (dashed black line). **e** Echosounder profile showing the intact sidewall stratigraphy with key horizons R1 to R8, glacial debris lobe, as well as pockmark and pipe structures.
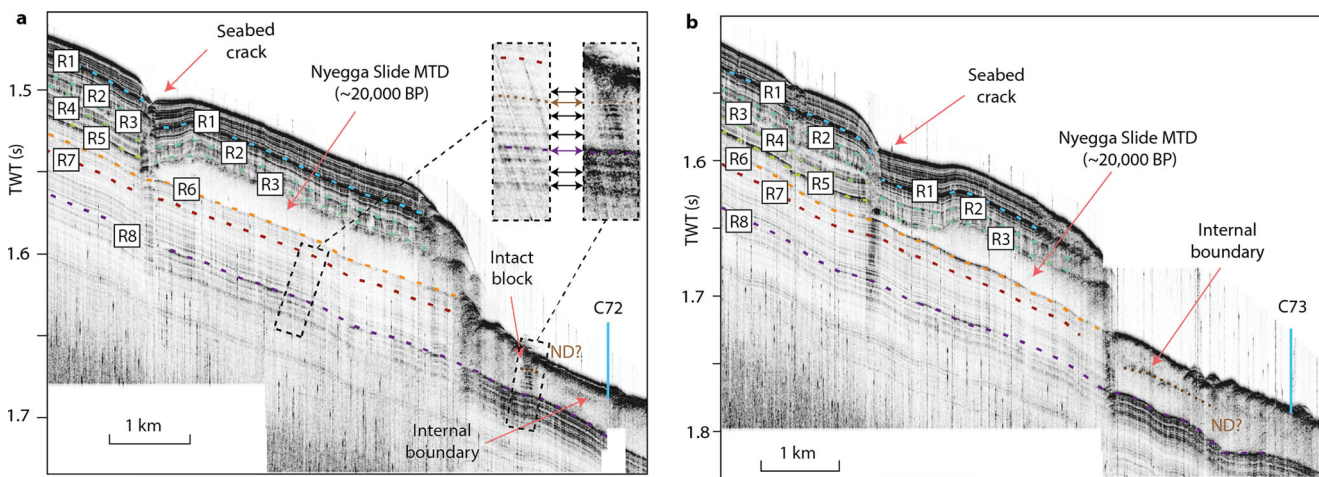

Fig. 3 Echosounder profiles from the sidewall of the Storegga Slide Complex. a and **b** Interpreted echosounder profiles crossing the northern Storegga Slide sidewall. R1 to R7 indicate the key reflections of the chrono-stratigraphic framework from Fig. 2a. The profiles show a partly buried ~ 20,000 BP Nyegga Slide MTD, the projected sediment core locations, and the slide scar infill with indications for an internal boundary (Nyegga discontinuity, marked with ND), and the key horizons R1 to R8. Enlargements show a comparison between the stratigraphy of the sidewall and an intact block.
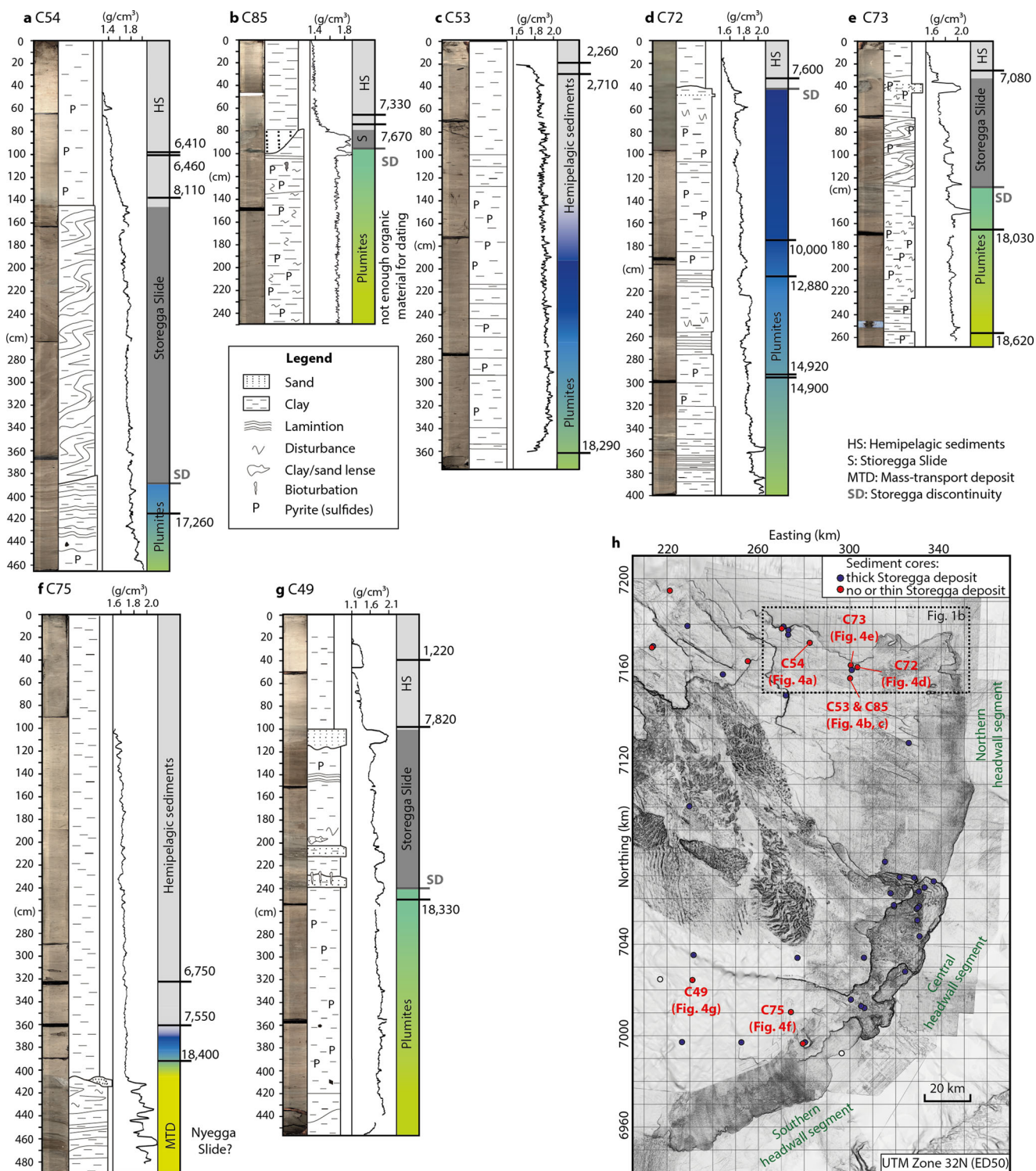
Fig. 4 Compilation of sediment cores penetrating the Storegga discontinuity (SD) with post-LGM deposits beneath. a–g Photographic and gamma-ray density scans, and visual core descriptions. Corrected radiocarbon derived ages were used to approximate the age-depth progression in the core, which is indicated by the coloration that matches the color scale in Fig. 2a. **h** Overview map showing the locations of the cores. For more detail see Supplementary Fig. S1.

found at 2.5 m depth below seafloor in core C73, which corresponds to ~22 m above R8 (Fig. 5b). In core C72, sediments with an age of ~18,600 BP are expected at ~4 m depth below seafloor based on the age progression of radiocarbon dates within the core (Fig. 5c). This again corresponds to ~22 m above R8 (Fig. 5a), implying that the relative stratigraphic depth of post-Nyegga Slide sediments is 35 to 37 m deeper in the slide scar than in the intact sidewall (Fig. 5). This is an indicative measure for the thickness of sediments that failed during the Nyegga Slide and implies that the Nyegga Slide failed along multiple glide planes, a feature that has also been observed for the Storegga Slide[4,6].
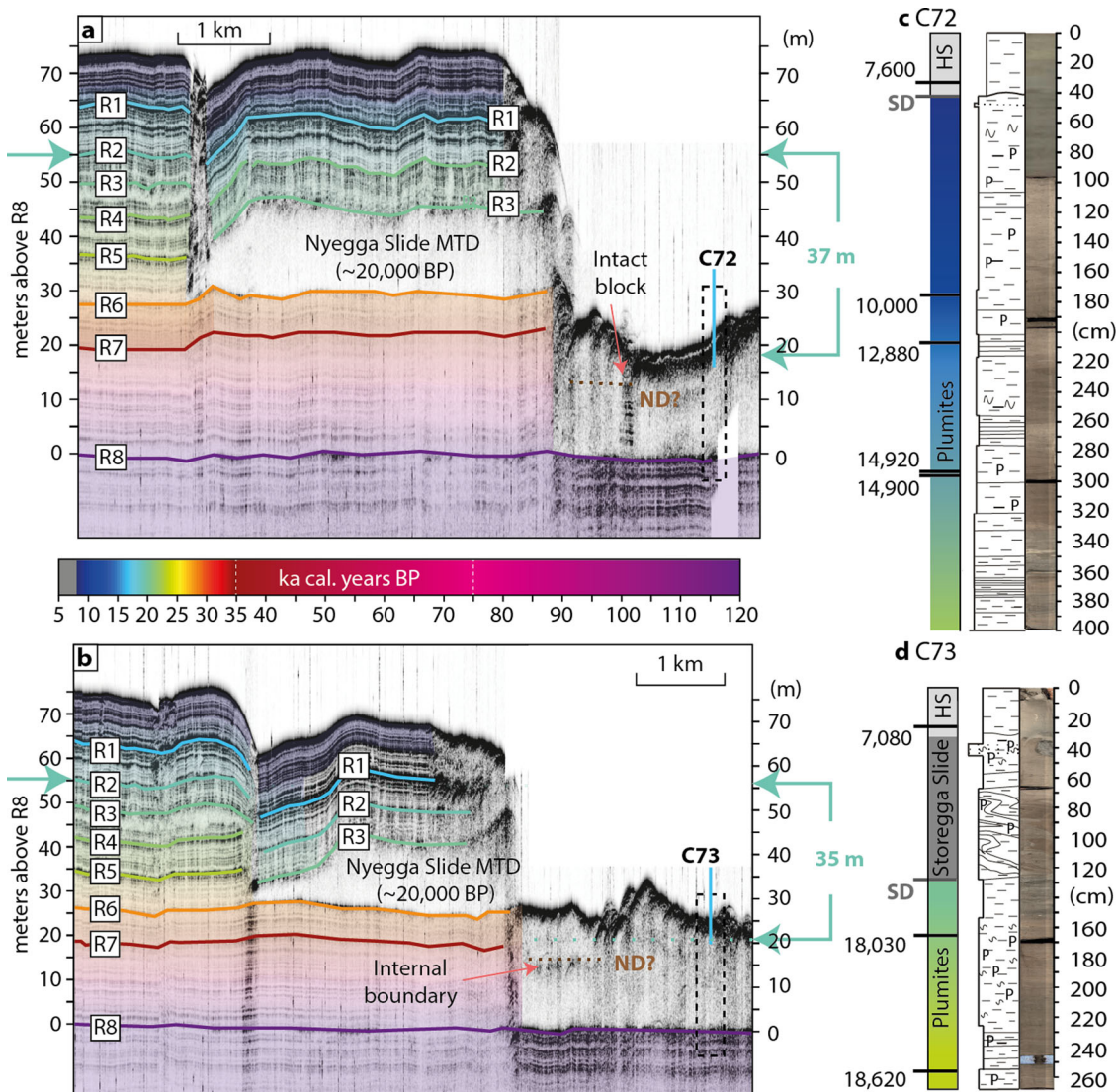
Fig. 5 Integration of the sidewall seismostratigraphy with sediment core chronostratigraphy from the north-eastern slide scar. a and **b** Flattened versions of the echosounder profiles from Fig. 3. The flattened profiles show a partly buried ~20,000 BP Nyegga Slide MTD, the projected sediment core locations, and the slide scar infill with indications for an internal boundary (Nyegga discontinuity, marked with ND), and the key horizons R1 to R8. Semi-transparent colour overlays in panels a and b illustrate the age depth model within the sediments (see colour bar between panels a and b). **c** and **d** Sediment cores C72 and C73 with radiocarbon sample (calendar ages). SD marks the Storegga Slide Discontinuity. Colours again correspond to the colour bar between panels a and b.

Only 11 cores penetrate the Storegga Slide deposit or discontinuity (seven presented in Fig. 4; all marked in Supplementary Fig. S1) and all show either post-LGM deposits beneath, or a continuous age progression from the Holocene to the phase after the LGM. The sedimentological record in these cores can only be explained by a revised slope failure history for the Storegga Slide Complex. Cores that terminate in Storegga Slide deposits, i.e. all those in the central segment (Supplementary Fig. S1), clearly illustrate the ~8150 BP event, but they provide no information on earlier events as the Storegga discontinuity was not penetrated. None of the cores that penetrate the Storegga deposits or discontinuity shows deposits older than the LGM, which would be expected if the scarp had been formed solely by the Storegga Slide.

Discussion

Revised slope failure history. Based on the presented observations of the Storegga area, we suggest an updated reconstruction of the present-day slide scar (Fig. 6b). At ~20,000 BP, more than 35 m of rapidly deposited and presumably poorly consolidated glacial sediments failed during the Nyegga Slide. The Nyegga slope failure mobilized sediments deposited between >30,000 and ~20,000 BP, forming the Nyegga discontinuity (ND) that likely corresponds to the internal boundary in the deposits in the northern sidewall and the top of the intact block in the slide scar infill (between R7 and R8 in Fig. 5a, b). After the LGM, the sediment-rich melt-water plumes deposited ~25 m of poorly consolidated sediments onto the entire study area, including the slide scar[13,14]. At ~8150 BP, parts of the sediments deposited after the LGM failed during the first phase of the Storegga Slide, forming the Storegga discontinuity, which was followed by lateral spreading of the remaining slide scar infill along a much deeper glide plane coinciding with R8 (Figs. 2 and 3) and the tsunami-genic failure of the central slide segment. Although the amount of slide scar evacuation during the Storegga Slide is substantially reduced through the recognition of the Nyegga Slide, the general
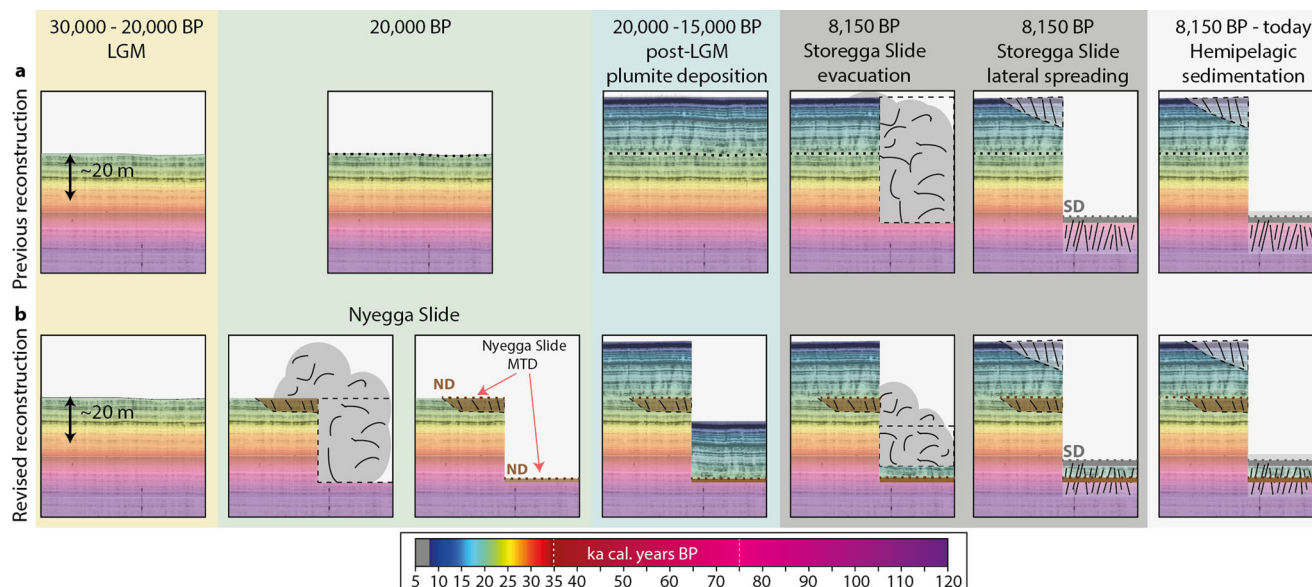
Fig. 6 Comparison between the previous and revised reconstruction of slope failure. a The "previous reconstruction" assumes that the NE slide scar evacuation occurred solely during the 8,150 BP Storegga Slide event and removed all sediments younger than 30,000 years. **b** The revised reconstruction (this study) shows that most of the slide scar evacuation occurred during the ~20,000 BP Nyegga Slide event and that the Storegga Slide only removed parts of the post-LGM sediment cover. Colour shading-age relationship is the same as defined in Fig. 2a and is shown again here (bottom).

chain of events during the Storegga Slide is in agreement with that of previous interpretations[4,6]. Loss of support and seismic loading, which were identified as main triggering mechanisms for lateral spreading in the Storegga Slide Complex[16], are also plausible triggering mechanisms to have affected the slopes during the Nyegga Slide. In this case, the Nyegga Slide included the disintegration of the shallow sedimentary column forming debris flows as well as lateral spreading of the remaining sediments. However, based on the available data, it is not possible to determine whether lateral spreading initiated during the Nyegga Slide and was then reactivated during the Storegga Slide, or whether it first initiated with the Storegga Slide. Our echosounder dataset covers only the northern boundary of Storegga Slide complex, and the presented seismostratigraphic analysis is only possible here as glacial debris lobes prevent seismic horizons from being correlated along the headwall (Fig. 1). Consequently, it is difficult to constrain whether the Nyegga Slide was a local event limited to the northern margin of the slide scar, or a regional event. However, at least three sediment cores from the southern slide scar segment also show indications for LGM slope failure, with C49 showing ~18,000 BP sediments beneath Storegga Slide deposits and C75 even including LGM mass-transport deposits (Fig. 4f, g). While this may indicate that the Nyegga Slide affected the entire Storegga Slide scar area, this is far from certain due to a lack of conclusive evidence for large stretches of slide scar. Based on the available data, we observe that ~70% of the 50 m that failed at the northern margin of the scar failed during the Nyegga Slide, and not during the Storegga Slide, indicating that the Nyegga Slide was a major failure event. The echosounder data and sediment cores also suggest a major slope failure at the end of the LGM along the southern slide scar segments. The northern and southern areas in which the new data suggest failure are ~200 km apart. While it is possible that there were two separate events, this seems unlikely because there are no clear morphological segmentations within the region, apart from the deep central incision that unequivocally belongs to the Storegga Slide (Supplementary Fig. S1). Additionally, it is unlikely that there were two almost simultaneous slides in close proximity that occurred without affecting each other. Assuming that there was only one major

slide at the end of the LGM, and considering that 70% of slide scar evacuation at the northern side wall occurred during the ~20,000 BP slope failure, it is possible to estimate the volume of the Nyegga Slide. Applying this percentage (70%) to the ~1300 to 1600 km³ of the initial phase of the Storegga Slide results in a Nyegga Slide volume of 900 to 1100 km³. In this case, the Nyegga Slide would have had dimensions similar to the ~900 km³ Trænadjupet Slide[17] or the 1250 km³ Hinlopen Slide[18]. It would also reduce the volume of the Storegga Slide to 1300 to 2300 km³.

Implications for slope failure and tsunami hazard along the North Atlantic Margin. Our proposed reduction of the Storegga Slide volume is not in conflict with the well-constrained tsunami observations as it does not affect the deeply incised failure of the central slide scar segment, which is considered the main source of the tsunami[7]. Our data are inconclusive about whether the Nyegga Slide occurred in one large or several small-scale events. Assuming slope failure associated with the Nyegga Slide occurred in one phase, it is likely that the event triggered a large regional tsunami. However, as sea-level was ~130 m lower during the LGM compared to today, and because surrounding coasts were mainly glaciated, tsunami deposits of this event are not expected to be preserved.

Processes preconditioning slope failure in the study area have been studied extensively in respect to the Storegga Slide[5]. Preconditioning processes include gas hydrate dissociation[19,20], elevated pore pressure due to rapid loading by glacial sediments[5], and ice-sheet dynamics[21]. All these destabilising factors were amplified during or shortly after the LGM compared to ~8150 BP: The analysis of gas hydrate dynamics beneath the Nyegga Pockmark field revealed pronounced gas hydrate redistribution and related active seafloor fluid flow during the LGM in an area directly next to the study area[14] (pockmarks and pipes in Figs. 1 and 2e). The presence of free gas has the potential to reduce the effective stress in marine sediments and may contribute to a reduction of slope stability[22]. Peak sedimentation rates greater than 12 m/kyrs during the LGM caused excess pore pressure[23], which would have the potential to precondition slope failures[24,25]. Unloading by ice-stream retreat from the headwall of the slide

complex induced excess pore pressure in shallow sediments and additionally caused loading-controlled tilting of the slope[21]. An additional potential trigger of slope failure is the deposition of glacial debris lobes at the shelf edge. Numerical simulations from the Storfjorden Trough Mouth Fan suggest that porosity and permeability contrasts between glacial debris flows and plumites favour the accumulation of pore overpressure and potentially precondition slope failure, when lower permeability glacial debris lobes cover higher permeability plumite layers[26]. Such a configuration at the end of the LGM in the Storegga region, as imaged in Fig. 2e, could explain fluid overpressure accumulation and the development of a weak layer in sediment layers beneath R4, which were affected by the ~20,000 BP slope failure. Based on our chrono-stratigraphic framework, glacial debris flows reached the area around 21,000 BP (R4 in Fig. 2b) and were interbedded within the undisturbed stratigraphy. Although the MTD inter-bedded within the sidewall is located more than 20 km down-slope, it is possible that it represents debris lobe material. However, the MTD formation occurred ~1000 years later than debris lobe deposition further upslope, and its emplacement has removed material from the stratigraphy (Fig. 3b), in contrast to the glacial debris lobes at the shelf edge (Fig. 2b). Therefore, failure of debris lobes at the shelf edge in response to ice retreat (as observed at the Storfjorden and Kveithola Trough-Mouth Fans in the Barents Sea[27]) is one of the most plausible triggers for the Nyegga Slide, and the distinct topographic step at the headwall (Fig. 2c) may represent evidence for this.

The evacuation of most LGM sediments from the slide scar long before the Storegga Slide makes Storegga preconditioning even more enigmatic, since large amounts of potentially unstable sediment were already removed by the Nyegga Slide. Our reinterpretation suggests that the focus for understanding the Storegga Slide should turn to its deeply-incised central slide segment, which correlates spatially with the Ormen Lange gas field. It is likely that focused fluid flow[28] played a similarly important role in the Storegga Slide as for slope failures at other continental slope margins[24,29].

As the Storegga Slide is considered the best-studied mega-slide complex in the world and has been used as a benchmark for slide emplacement and tsunami generation by submarine landslides, our findings call for a re-evaluation of studies that assess geohazards based on Storegga Slide insights, e.g. ref. [30]. The identification of the Nyegga Slide indicates that large-scale slope failures occur more frequently than previously assumed. Instead of one major landslide per glacial cycle there were at least two in the Storegga Slide area. Regardless of whether there were one or two major slides affecting the northern and southern Storegga Slide region at the end of the LGM, or only one Nyegga Slide, our results suggest that the Storegga Slide was at least 30% smaller than previously stated, but was still able to generate the observed devastating basin-wide tsunami. This reconciles the observed run-up heights and tsunami simulations[7] that suggested that the failure of the central part of the Storegga Slide was the main contributor of the Storegga tsunami. The more frequent occurrence of major landslides indicates an increased tsunami hazard for the North Atlantic. Hence, risk assessments, tsunami models for the Storegga Slide, and studies that are based on the Storegga Slide by proxy, require a revised parameterization.

Methods

Echosounder and bathymetric data. Our analysis is based on different geophysical datasets. The sub-bottom profiler data were acquired during research cruise M87/2 on board research vessel RV Meteor in 2012 using a Teledyne Parasound system (Figs. 2–4). The bathymetric dataset used in this study is a compilation of the regional bathymetric grid created by partners of the Seabed project based on data provided by Norsk Hydro AS, detailed bathymetry grids from the Mareano database provided by Norwegian Mapping Authority Hydrographic Service and 3D

seismic seafloor picks. The datasets were combined and analysed using the seismic interpretation software Kingdom Suite by HIS and Petrel by Schlumberger.

Sedimentological core analysis. The sediment cores have been analysed primarily as part of the Ormen Lange Project[4,8]. We re-analysed existing core descriptions for ambiguous interpretations and re-analysed seven cores in detail (Supplementary Fig. S1). The radiocarbon dates we used were corrected for global effects using the Marine20 dataset[31] and are shown in Supplementary Table S1.

References
1. Fine, I. V., Rabinovich, A. B., Bornhold, B. D., Thomson, R. E. & Kulikov, E. A. The Grand Banks landslide-generated tsunami of November 18, 1929: preliminary analysis and numerical modeling. *Mar. Geol.* **215**, 45–57 (2005).
2. Twichell, D. C., Chaytor, J. D., Uri, S. & Buczkowski, B. Morphology of late Quaternary submarine landslides along the US Atlantic continental margin. *Mar. Geol.* **264**, 4–15 (2009).
3. Evans, D. et al. Palaeoslides and other mass failures of Pliocene to Pleistocene age along the Atlantic continental margin of NW Europe. *Mar. Pet. Geol.* **22**, 1131–1148 (2005).
4. Haflidason, H. et al. The Storegga Slide: architecture, geometry and slide development. *Mar. Geol.* **213**, 201–234 (2004).
5. Bryn, P., Berg, K., Forsberg, C. F., Solheim, A. & Kvalstad, T. J. Explaining the Storegga slide. *Mar. Pet. Geol.y* **22**, 11–19 (2005).
6. Micallef, A., Masson, D. G., Berndt, C. & Stow, D. A. Development and mass movement processes of the north-eastern Storegga Slide. *Quat. Sci. Rev.* **28**, 433–448 (2009).
7. Løvholt, F., Harbitz, C. B., & Haugen, K. B. *A parametric study of tsunamis generated by submarine slides in the Ormen Lange/Storegga area off western Norway. In Ormen Lange–an Integrated Study for Safe Field Development in the Storegga Submarine Area.* 219–231 (Elsevier, 2005).
8. Haflidason, H., Lien, R., Sejrup, H. P., Forsberg, C. F. & Bryn, P. The dating and morphometry of the Storegga Slide. *Marine and Pet. Geology* **22**, 123–136 (2005).
9. Bondevik, S. et al. The Storegga Slide tsunami—comparing field observations with numerical simulations. *Mar. Pet. Geol.* **22**, 195–208 (2005).
10. Wagner, B., Bennike, O., Klug, M. & Cremer, H. First indication of Storegga tsunami deposits from East Greenland. *J. Quat. Sci.* **22**, 321–325 (2007).
11. Romundset, A. & Bondevik, S. Propagation of the Storegga tsunami into ice-free lakes along the southern shores of the Barents Sea. *J. Quat. Sci.* **26**, 457–462 (2011).
12. Fruergaard, M. et al. Tsunami propagation over a wide, shallow continental shelf caused by the Storegga slide, southeastern North Sea, Denmark. *Geology* **43**, 1047–1050 (2015).
13. Reiche, S., Hjelstuen, B. O. & Haflidason, H. High-resolution seismic stratigraphy, sedimentary processes and the origin of seabed cracks and pockmarks at Nyegga, mid-Norwegian margin. *Mar. Geol.* **284**, 28–39 (2011).
14. Karstens, J. et al. Glacigenic sedimentation pulses triggered post-glacial gas hydrate dissociation. *Nat. Commun.* **9**, 635 (2018).
15. Solheim, A., Berg, K., Forsberg, C. F. & Bryn, P. The Storegga Slide complex: repetitive large scale sliding with similar cause and development. *Mar. Pet. Geol.* **22**, 97–107 (2005).
16. Micallef, A., Masson, D. G., Berndt, C., & Stow, D. A. Morphology and mechanics of submarine spreading: A case study from the Storegga Slide. *J. Geophys. Res. Earth Surf.* **112**, F000739 (2007).
17. Laberg, J. S. & Vorren, T. O. The Trænadjupet Slide, offshore Norway—morphology, evacuation and triggering mechanisms. *Marine Geology* **171**, 95–114 (2000).
18. Geissler, W. H. et al. Arctic megaslide at presumed rest. *Sci. Rep.* **6**, 1–8 (2016).
19. Jung, W. Y., & Vogt, P. R. Effects of bottom water warming and sea level rise on Holocene hydrate dissociation and mass wasting along the Norwegian-Barents Continental Margin. *J. Geophys. Res. Solid Earth.* **109**, B002738 (2004).

20. Mienert, J. et al. *Ocean warming and gas hydrate stability on the mid-Norwegian margin at the Storegga Slide. In Ormen Lange–an Integrated Study for Safe Field Development in the Storegga Submarine Area*. 233–244 (Elsevier, 2005).
21. Urlaub, M., Kratzke, I. & Hjelstuen, B. O. A numerical investigation of excess pore pressures and continental slope stability in response to ice-sheet dynamics. *Geol. Soc. London, Spec. Publ.* **500**, 255–266 (2020).
22. Kaminski, P., Urlaub, M., Grabe, J. & Berndt, C. Geomechanical behaviour of gassy soils and implications for submarine slope stability: a literature analysis. *Geological Soc. London, Spec. Publ.* **500**, 277–288 (2020).
23. Hustoft, S., Bünz, S., Mienert, J. & Chand, S. Gas hydrate reservoir and active methane-venting province in sediments on < 20 Ma young oceanic crust in the Fram Strait, offshore NW-Svalbard. *Earth Planet. Sci. Lett.* **284**, 12–24 (2009).
24. Bellwald, B. et al. NE Atlantic continental slope stability from a numerical modeling perspective. *Quat. Sci. Rev.* **203**, 248–265 (2019).
25. Bailey, L. P. et al. Preconditioning by sediment accumulation can produce powerful turbidity currents without major external triggers. *Earth Planet. Sci. Lett.* **562**, 116845 (2021).
26. Llopart, J. et al. Fluid flow and pore pressure development throughout the evolution of a trough mouth fan, western Barents Sea. *Basin Res.* **31**, 487–513 (2019).
27. Lucchi, R. G. et al. *Recent submarine landslides on the continental slope of Storfjorden and Kveithola Trough-Mouth Fans (north west Barents Sea). In Submarine mass movements and their consequences* 735–745 (Spreinger, 2012).
28. Bünz, S., Mienert, J., Bryn, P. & Berg, K. Fluid flow impact on slope failure from 3D seismic data: a case study in the Storegga Slide. *Basin Res.* **17**, 109–122 (2005).
29. Elger, J. et al. Submarine slope failures due to pipe structure formation. *Nat. Commun.* **9**, 1–6 (2018).
30. Berndt, C., Brune, S., Nisbet, E., Zschau, J., & Sobolev, S. V. Tsunami modeling of a submarine landslide in the Fram Strait. *Geochem. Geophys. Geosyst.* **10**, 4 (2009).
31. Heaton, T. J. et al. Marine20—the marine radiocarbon age calibration curve (0–55,000 cal BP). *Radiocarbon* **62**, 779–820 (2020).

Acknowledgements

Author contributions

J.K., G.C. and C.B. were responsible for the acquisition, processing and interpretation of the echosounder profiles. J.K. and H.H. were responsible for the analysis and interpretation of the sediment cores. J.K., H.H., C.B. and G.C. integrated and interpreted the datasets and wrote the manuscript.

Funding

Competing interests

The authors declare no competing interests.

Additional information

Supplementary information The online version contains supplementary material available at https://doi.org/10.1038/s43247-023-00710-y.

Correspondence and requests for materials should be addressed to Jens Karstens.

Peer review information *Communications Earth & Environment* thanks Renata Giulia Lucchi, Maarten Vanneste and Derek Sawyer for their contribution to the peer review of this work. Primary Handling Editors: João Duarte and Joe Aslin. Peer reviewer reports are available.

Reprints and permission information is available at http://www.nature.com/reprints

Publisher's note Springer Nature remains neutral with regard to jurisdictional claims in published maps and institutional affiliations.